



Comparison of UVC-based advanced oxidation processes in the mineralization of bisphenol A: Identification of oxidation by products and toxicity evaluation

Isaac Sánchez-Montes^a, Naihara Wachter^a, Bianca F. Silva^b, José M. Aquino^{a,*}

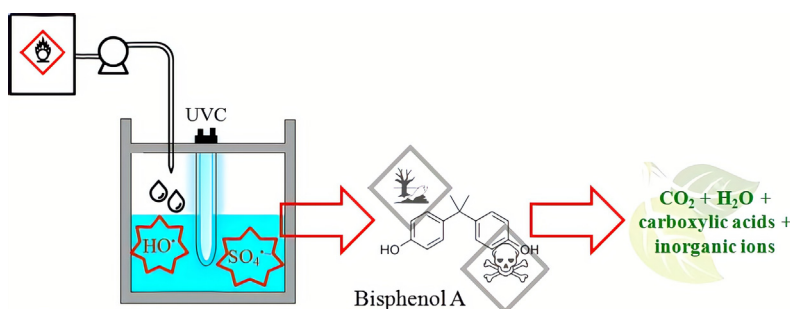
^a Departamento de Química, Universidade Federal de São Carlos, C.P. 676, 13560-970 São Carlos SP, Brazil

^b Instituto de Química de Araraquara, Departamento de Química Analítica, Universidade Estadual Paulista, 14800-900 Araraquara SP, Brazil

HIGHLIGHTS

- UVC/HOCl, UVC/S₂O₈²⁻, and UVC/H₂O₂ processes were assessed for bisphenol A removal.
- UVC irradiation led to production of HO•/SO₄•⁻ SO₄ species boosting conversion to CO₂.
- High mineralization rates were only attained using the UVC/HOCl method.
- Oxidation by-products might be responsible for the toxicity towards *Artemia salina*.
- UVC/HOCl method is the best choice as it allows high CO₂ conversion rates at lower costs.

GRAPHICAL ABSTRACT



ARTICLE INFO

Keywords:

Plasticizers
Synthetic organic compounds
Hydroxylation reactions
Advanced oxidation processes
UVC irradiation
Synergistic effect

ABSTRACT

Water contamination by contaminants of emerging concern (CEC) represents a major challenge to our society regarding the need to assure a high quality drinking water to prevent humans from developing health problems. Thus, the performance of three different advanced oxidation processes (AOP: UVC/HOCl, UVC/S₂O₈²⁻, and UVC/H₂O₂) based on the homolysis of oxidants were investigated for the oxidation and mineralization of bisphenol A (BPA) containing solutions as well as assessment of biotoxicity and identification of oxidation by-products. In all AOP, UVC irradiation led to a significant improvement for the oxidation and mineralization of BPA due to the production of HO•/SO₄•⁻ species. UVC/HOCl method was able to achieve high rates of conversion of BPA and its oxidation by-products to CO₂. All detected oxidation by-products resulted from hydroxylation reactions. Considering the short chain carboxylic acids, mainly produced after opening the aromatic ring, high concentrations appeared mainly during the first two hours of treatment for the UVC/HOCl method with a complete elimination within 6 h of treatment, including the dichloroacetic acid. Biotoxicity assays using *Artemia salina* crustacean showed that the mortality was ceased after 4 h of treatment using the UVC/HOCl and UVC/S₂O₈²⁻ processes. In contrast, a low mortality decrease was observed when using the UVC/H₂O₂ process, probably due to the accumulation of toxic intermediates. In all scenarios, toxicity of the BPA compound and its oxidation by-products seem to be responsible for the distinct decays of mortality, as confirmed on the ECOSAR software. Finally, the UVC/HOCl method is an interesting option to eliminate CEC for removing levels attained and energy consumption.

* Corresponding author.

E-mail address: jmaquino@ufscar.br (J.M. Aquino).

<https://doi.org/10.1016/j.cej.2019.123986>

Received 10 October 2019; Received in revised form 12 December 2019; Accepted 28 December 2019

Available online 31 December 2019

1385-8947/ © 2019 Elsevier B.V. All rights reserved.

1. Introduction

Many studies have reported the frequent toxic effect of some organic contaminants of emerging concern (CEC), such as pharmaceuticals, pesticides, personal care products, found in different sources of water [1–3]. These findings emphasize the necessity to remove, inactivate, or transform CEC into less toxic by-products than the initial compound before their disposal into the environment [4–6]. Among the available methods to treat contaminated solutions, investigations have increasingly focused on the ultraviolet-based advanced oxidation processes (UV/AOP) for the production of a large variety of short-lived radicals, e.g., hydroxyl (HO^\bullet), chlorine (Cl^\bullet), carbonate ($\text{CO}_3^{\bullet-}$), sulfate ($\text{SO}_4^{\bullet-}$), quite feasible leading to high elimination rates of organic pollutants at ambient temperature and pressure [5,7–14].

UVC/hydrogen peroxide (UVC/ H_2O_2) has been extensively used as an AOP for degradation of organic pollutants and water disinfection [9,15]. In this process, the non-selective HO^\bullet species can be produced from the homolytic cleavage of H_2O_2 through UVC radiation absorption (200–280 nm), as shown in Eq. (1), with a quantum efficiency at 254 nm ($\Phi_{254, \text{H}_2\text{O}_2}$) as low as 0.5 mol Es^{-1} [16–19]. Because of its high oxidizing power ($E^\circ_{\text{HO}^\bullet/\text{H}_2\text{O}} = 1.8 - 2.7 \text{ V}$) [20], HO^\bullet can react non-selectively with various organic compounds through electron transfer, hydrogen abstraction or electrophilic addition mechanisms at near diffusion-controlled rates [21].

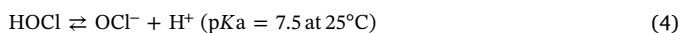


Recently, AOP based on sulfate radical ($\text{SO}_4^{\bullet-}$) has been proposed as an alternative method to remove recalcitrant organic compounds for its very high oxidation potential

($E^\circ_{\text{SO}_4^{\bullet-}/\text{SO}_4^{2-}} = 2.5 - 3.1 \text{ V}$) [20,22] possibly to develop through the activation of persulfate or peroxymonosulfate precursors through heat, UV irradiation, and transition-metal species [10,23]. In the case of UVC activation, particularly at 254 nm, the production of $\text{SO}_4^{\bullet-}$ species also occurs through a homolytic cleavage reaction (see Eq. (2)), which has a quantum yield efficiency 280% higher than with the use of H_2O_2 ($\Phi_{254, \text{S}_2\text{O}_8^{2-}} \sim 1.4 \text{ mol Es}^{-1}$) [24,25]. Consequently, high amounts of $\text{SO}_4^{\bullet-}$ species are generated, which can react with H_2O molecules resulting in the production of HO^\bullet species (see Eq. (3)). These electrophilic species can also react with aromatic compounds through three main mechanisms: *i*) radical adduct formation, *ii*) hydrogen atom abstraction, and *iii*) single electron transfer [23,26–28]. In addition, depending on the properties of the electron donating/withdrawing functional groups in the aromatic compound, the $\text{SO}_4^{\bullet-}$ species can lead to high oxidation rates of specific contaminants [28].



Active chlorine (represented by Cl_2 , HOCl , and OCl^-) are the most frequent oxidizing species in solutions used to deactivate dangerous pathogens [29–31] due to their medium to high oxidation power, low cost, and high accessibility compared to other reactive oxygen species used in AOP. The HOCl species is a weak acid that can co-exist in aqueous solution with its conjugate base (OCl^-), according to the equilibrium reaction shown in Eq. (4). The relative concentration of each species is strongly dependent on many variables, such as pH – so that at medium to low pH (3–7), HOCl is the main species [32].



The HOCl can be also used to produce HO^\bullet through a homolysis reaction in combination with a UVC source, as demonstrated in Eq. (5); however, the simultaneous formation of chlorine radical (Cl^\bullet), which might be so effective to oxidation and degradation of pollutants ($E^\circ_{\text{Cl}^\bullet/\text{Cl}^-} = 2.41 \text{ V}$) [33] as HO^\bullet and $\text{SO}_4^{\bullet-}$ species, can produce chlorinated intermediate compounds as the main drawback. According to Chuang

et al. [34], the UVC/ HOCl method achieves a higher HO^\bullet production than the UVC/ H_2O_2 process due to its superior quantum efficiency ($\Phi_{254, \text{HOCl}} \sim 1.5 \text{ mol Es}^{-1}$) [32,35]. Consequently, the energy requirements to treat solutions containing organic pollutants using the UVC/ HOCl method can be significantly lower.



The residual amount of HOCl after treatment using the UVC/ HOCl process is not a concern since a final post-chlorination step is usually required for water disinfection against regrowth of bacteria and external contamination [31].

Even though previous studies had investigated the efficiency of different UVC/AOP using distinct oxidizing agents [36–39], such as H_2O_2 , $\text{S}_2\text{O}_8^{2-}$, free chlorine, and HSO_5^- , to the best of our knowledge none of those works compare the performances of UVC/ H_2O_2 , UVC/ $\text{S}_2\text{O}_8^{2-}$ and UVC/ HOCl processes in terms of total organic carbon (TOC) removal, identification of oxidation by-products (long and short chain), and particularly toxicity evolution during treatment. Thus, we aimed at investigating the degradation and mineralization (conversion to CO_2) levels and rates of synthetic solutions of bisphenol A (BPA) using the above-mentioned UVC/AOP processes, *i.e.* UVC/ H_2O_2 , UVC/ $\text{S}_2\text{O}_8^{2-}$ and UVC/ HOCl homogeneous processes. We will assess and compare the possible synergistic effects through experiments using only the UVC lamp (photochemical process) or addition of oxidants (chemical process). To investigate the main susceptible sites to the addition reactions generated from the electrophilic HO^\bullet species in the BPA molecule, high-performance liquid chromatography (HPLC) will monitor the BPA concentration evolution, main generated short-chain carboxylic acids, and long chain oxidation by-products coupled to mass spectrometry. Finally, we will assess and compare the toxicity evolution of the treated solutions towards *Artemia salina*, an aquatic crustacean, with the oxidation by-product compounds and TOC removal found.

2. Materials and methods

2.1. Chemicals

All chemicals were used without further purification, including BPA (99%, Sigma Aldrich), H_2O_2 (29–31%, Synth), $\text{Na}_2\text{S}_2\text{O}_8$ (a.r., Sigma Aldrich), NaOCl (10–12%, Nalgon), H_3PO_4 (85%, Mallinckrodt), $\text{Na}_2\text{S}_2\text{O}_3$ (a.r., Qhemis), KI (a.r., Sigma Aldrich), NaOH (a.r., Synth), H_2SO_4 (a.r., Mallinckrodt), NH_4OH (28–30%, Macron), ethanol (99.5%, Synth), isopropanol (99.5%, Qhemis), tert-butyl alcohol (99%, Exodo), benzoic acid (a.r., Sigma Aldrich), salicylic acid (a.r., Sigma Aldrich), acetonitrile (HPLC grade, JT Baker), and short-chain carboxylic acids (a.r., Sigma Aldrich). The preparation of all solutions used deionized water (Millipore Milli-Q system, $\rho \geq 18.2 \text{ M}\Omega \text{ cm}$).

2.2. Degradation experiments

UVC/AOP experiments for oxidation of BPA (0.44 mmol L^{-1}) solutions were carried out using a glass vessel of 1.5 L equipped with a magnetic stirrer and a quartz tube. A 9 W UVC lamp (main emission line at 253.7 nm from Phillips) with a fluency rate of 20.2 mW cm^{-2} (details on the fluency rate calculation and other information are available in the supplementary file of a previous work [14]) was inserted inside the tube (see Fig. S1 in the supplementary file). Control experiments were carried out using only the oxidants (H_2O_2 , $\text{Na}_2\text{S}_2\text{O}_8$, or HOCl – chemical method) or UVC lamp (photochemical method) to better understand the synergistic effect resulting from coupling these methods. As the literature reports [40–47], the use of high initial oxidant concentrations in UVC/AOP leads to recombination reactions of radicals, thus reducing their efficiency in the CEC degradation and mineralization (see rate constants for some self-scavenging reactions in Table S1, in the supplementary information file). To avoid these undesirable reactions, we

continuously added freshly prepared solutions of the oxidants (0.6 mol L^{-1}) to the reaction vessel during the experiments at a flow rate of 0.1 mL min^{-1} using a peristaltic pump (Gilson Miniplus 3). The solution pH was maintained around 3.0 by adding concentrated H_2SO_4 or NaOH solutions. Other operational variables, such as treatment time, solution temperature, and solution volume, were maintained fixed at 360 min, $38 \text{ }^\circ\text{C}$, and 1.0 L, respectively. Before further analyses and to avoid oxidation from any residual oxidant, a few drops of a concentrated reducing solution of $\text{Na}_2\text{S}_2\text{O}_3$ to BPA extracted samples containing solution.

2.3. Analyses

The concentration evolution of BPA (detected at 280 nm) was monitored through high-performance liquid chromatography (HPLC) using a core-shell C-18 reversed phase as the stationary phase (Phenomenex®: 150 mm \times 4.6 mm, 5 μm particle, 100 Å) and a mixture of aqueous 0.1% (V/V) formic acid and acetonitrile (60:40 V/V) in an isocratic elution mode as the mobile phase, at 1.0 mL min^{-1} . The injection volume and temperature of the column were 25 μL and $23 \text{ }^\circ\text{C}$, respectively. For analysis purposes, the BPA removal during the UVC/AOPs processes is expressed in its remaining fraction, i.e. as $x_{\text{BPA}}^{\text{rem}} = [\text{BPA}]_t/[\text{BPA}]_0$, in which $[\text{BPA}]_t$ and $[\text{BPA}]_0$ are the values at time t and prior to the experiment, respectively.

Analyses of liquid chromatography coupled to a mass spectrometer (LC-MS/MS) determined the intermediates produced during BPA degradation. For this purpose, samples (2 mL) were collected at predetermined times, filtered using a 0.22 μm polypropylene cartridge coupled to a glass syringe and injected without any further preparation. The analyses were performed in a 1200 Agilent Technologies HPLC coupled to a 3200 QTRAP mass spectrometer (QqLIT – Linear Ion Trap Quadrupole LC-MS/MS Mass Spectrometer), AB SCIEX Instruments, operating in a negative mode, and TurboIonSpray ionization. The software Lightsight® 2.3 (Nominal Mass Metabolite ID Software, AB SCIEX) was used to investigate all possible by-products after optimizing the ionization and fragmentation parameters for the initial compound. These parameters were obtained using a direct infusion of $10 \mu\text{L min}^{-1}$ of a solution containing BPA (0.44 mmol L^{-1}) in ACN:H₂O (1:1 V/V) with 0.1% of ammonium hydroxide. The MS/MS conditions were: curtain gas at 20 psi, ion spray at -4500 V , gas 1 and gas 2 at 50 psi, temperature of $650 \text{ }^\circ\text{C}$, interface heater on, declustering potential, entrance potential, and cell entrance potential were of -50 , -9.5 , and -21 V , respectively. Optimized selected multiple reaction monitoring (SRM) and fullscan experiments were performed automatically on the LightSight® software. Different types of reactions were investigated, such as oxidation, hydroxylation, reduction, C–C bond cleavage, chlorination, among others. During the MS/MS experiments, the HPLC analyses were performed as aforementioned, but with the addition of an injection volume of 20 μL and ammonium hydroxide into the H₂O component of the mobile phase to reach a final concentration of 0.1% (V/V).

The short chain carboxylic acids were also determined during the degradation experiments through HPLC using a Rezex™ ROA-H column (Phenomenex®: 300 mm \times 7.8 mm, 8 μm particle) as the stationary phase and a $2.5 \text{ mmol L}^{-1} \text{ H}_2\text{SO}_4$ solution as the mobile phase at 0.5 mL min^{-1} . Before these analyses, samples collected at predetermined times were filtered using a 0.22 μm polypropylene cartridge coupled to a glass syringe. The carboxylic acids (detected at 210 nm) were identified by comparison of their retention times with those of previously analyzed standards. The injection volume and column temperature were 25 μL and $23 \text{ }^\circ\text{C}$, respectively.

The concentration evolution of oxidants was determined by two different methods using a UV-Vis spectrophotometer (Shimadzu UV-1800). The iodometric method used to determine $\text{S}_2\text{O}_8^{2-}$ and HOCl concentrations was adapted from Liang et al. [48]. Briefly, 90 μL of a 0.093 mol L^{-1} ammonium molybdate solution and 140 μL of a 2.5 mol

L^{-1} KI solution were added to 3.5 mL of sample previously acidified with glacial acetic acid; subsequently, the samples were analyzed at 351 nm. The spectrophotometric method used to measure the H₂O₂ concentration, in turn, was adapted from Chai et al. (2004) [49] following a similar procedure, but without KI addition. In this case, the peroxomolybdate complex formed was spectrophotometrically measured at 350 nm.

The extent of mineralization (i.e. conversion to CO₂) was monitored through total organic carbon concentration ([TOC]) measurements using a GE Sievers Innovox analyzer. The [TOC] determination was carried out after mixing a diluted volume of the treated sample with H₃PO₄ (6 mol L^{-1}) and Na₂S₂O₈ (30% m/V) solutions. Further experimental details can be found elsewhere [14,50]. Once more, for analysis purposes, the removal of TOC during the treatment is expressed in its remaining fraction, i.e. as $x_{\text{TOC}}^{\text{rem}} = [\text{TOC}]_t/[\text{TOC}]_0$, in which $[\text{TOC}]_t$ and $[\text{TOC}]_0$ are the values at time t and prior to the experiment, respectively.

Acute toxicity assays were carried out using the crustacean *Artemia salina* (*A. salina*), whose main advantage is their tolerance to variable pH, temperature, and dissolved oxygen conditions in saline medium, despite being less sensitive than other testing organisms [51,52]. The tests were carried out according to the work of Vanhaecke et al. [53], with modifications, as described in another study by our group [54], using *A. salina* cysts from Maramar Brazil and synthetic sea salt from Red Sea. The toxicity tests were carried out in triplicate using glass tubes containing 10 mL of initial and treated samples after adding a few drops of Na₂S₂O₃ solution. Negative and positive controls contained artificial seawater (3.5% m/m) with 20.0 mmol L⁻¹ Na₂S₂O₃ and artificial seawater with varying concentrations of sodium dodecyl sulfate (SDS; 10.0, 13.5, 18.0, 24.0, and 32.0 mg L⁻¹), respectively. SDS, which is known as a reference toxicant for *A. salina*, was used to ensure the quality of the cysts and conducted experiments to determine the median lethal concentration (LC₅₀) of BPA at specific values (3.12, 6.25, 12.5, 25.0 and 50.0 mg L⁻¹ in artificial seawater 3.5% m/m). The LC₅₀ values for the SDS positive control and BPA compound followed the Trimmed Spearman-Kärber method [55]. The percentage of mortality was expressed by the ratio between the number of dead organisms and the total number of organisms.

It has been increasingly relevant to predict the toxicological effects of new chemical compounds and degradation by-products based on their chemical structure and physical properties since a trustworthy prediction can substitute experimental tests using animals. Thus, quantitative structure-activity relationships (QSARs) analysis through the ecological structure-activity relationship (ECOSAR) model [56–60] was conducted to demonstrate the baseline acute and chronic toxicity at three different trophic levels (i.e. fish, daphnid, and green algae) for the BPA molecule and by-products identified through LC-MS/MS analyses. The ECOSAR v1.11 program, developed by U.S. Environmental Protection Agency, can estimate toxicity of chemical compounds based on data from structurally similar chemical classes.

The extent of total mineralization (φ) was calculated through the ratio between the removal fractions of TOC and BPA after a given time of treatment and using Eq. (6) [61]:

$$\varphi = \frac{1 - x_{\text{TOC}}^{\text{rem}}}{1 - x_{\text{BPA}}^{\text{rem}}} \quad (6)$$

The φ value indicates the degree of BPA molecules conversion to CO₂ or other intermediate compounds, which can range from 0 to 1 – no mineralization or total mineralization of the oxidized BPA molecule, respectively.

Finally, an economic comparison between the investigated processes was performed based on the total cost per order of BPA or TOC removal, i.e. Cost/O_{TOTAL} ($\$ \text{ m}^{-3} \text{ order}^{-1}$), encompassing costs of electric energy (Cost/O_{UVC}) added with 45% of maintenance costs [62] and chemicals (Cost/O_{OX}), as shown in Eq. (7). The Cost/O_{UVC} ($\$ \text{ m}^{-3}$

order⁻¹) is determined by the electric energy (EE in kW) required to oxidize or mineralize the target pollutant by one order of magnitude in 1.0 m³ of water per order (O_{UVC}), as shown in Eqs. (8) and (9) [63]:

$$\text{Cost}/O_{\text{TOTAL}} = \text{Cost}/O_{\text{UVC}} + \text{Cost}/O_{\text{OX}} \quad (7)$$

$$\text{Cost}/O_{\text{UVC}} = 1.45 \times \frac{\text{EE}}{O_{\text{UVC}}} \times \text{electricity cost} \quad (8)$$

$$\frac{\text{EE}}{O_{\text{UVC}}} = \frac{2.303 P}{60 V k_{1st}} \quad (9)$$

where P is the lamp power output (i.e. fluency rate \times illuminated area of the reservoir = 20.2 mW cm⁻² \times 782 cm² = 15.8 W) or the rated power (9 W), t the reaction time (h), V the solution volume (m³), k the rate constant (pseudo-first order in min⁻¹), 2.303 is a conversion factor for logarithm, and 60 is another conversion factor (min h⁻¹). The average electricity cost is 0.1 \$ kW⁻¹h⁻¹ according to the Brazilian electricity regulatory agency in 2017.

3. Results and discussion

3.1. Oxidation and mineralization of BPA using distinct UVC/AOP

Firstly, control experiments were carried out to explore the extent of BPA oxidation (0.44 mmol L⁻¹) in aqueous solution using only UVC irradiation (photochemical method) or distinct oxidants (H₂O₂, Na₂S₂O₈, or HOCl – chemical method). Fig. 1 shows the evolution of the remaining fraction of BPA ($x_{\text{BPA}}^{\text{rem}} = [\text{BPA}]_t/[\text{BPA}]_0$) and TOC ($x_{\text{TOC}}^{\text{rem}} = [\text{TOC}]_t/[\text{TOC}]_0$) as a function of treatment time (t) for the photochemical and chemical methods at pH 3 and 38 °C. As illustrated in Fig. 1a, a significant BPA removal (55%) was achieved after 360 min using exclusively the UVC lamp. The BPA degradation through the UVC irradiation can be attributed to the absorption capacity of light by the BPA molecule, which is measured through the molar absorption coefficient ($\epsilon_{254, \text{BPA}} = 912 \text{ M cm}^{-1}$) and quantum yield ($\Phi_{254, \text{BPA}} = 0.0075 \text{ mol Es}^{-1}$). These two fundamental parameters drive the direct photolysis rate. Thus, under UVC irradiation, the BPA molecule absorbs emitted photons that are capable to induce electron state transitions resulting in the formation of excited BPA molecules (BPA*). These molecules may lose their excess energy after decomposition with the consequent generation of by-products. The chemical process using H₂O₂ and Na₂S₂O₈ as oxidant agent led to very low degradation rates even after 360 min, suggesting that the BPA molecule is recalcitrant towards oxidation using those chemicals. In contrast, the chemical

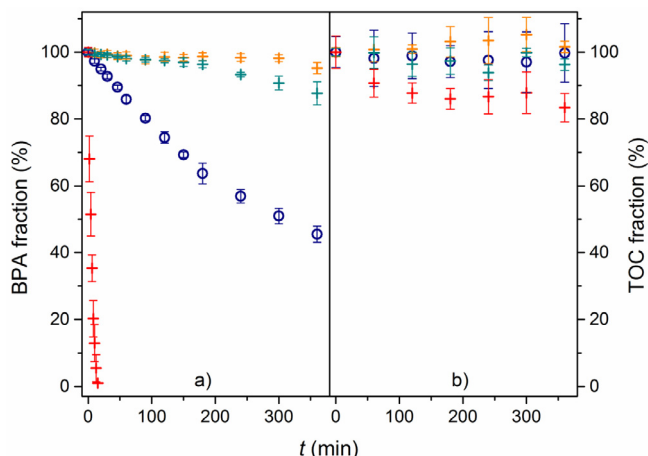


Fig. 1. Remaining a) BPA and b) TOC fraction as a function of treatment time for the photochemical (○) and chemical (H₂O₂ (+), S₂O₈²⁻ (Δ), and HOCl (□)) processes. Conditions: 0.6 mol L⁻¹ of oxidant (flow rate 0.1 mL min⁻¹), pH 3, and 38 °C. Error bars refer to two and three repetitions for the BPA and TOC determinations, respectively.

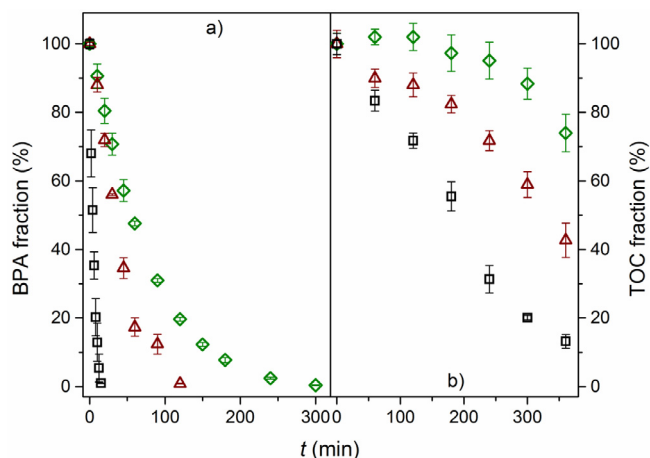


Fig. 2. Remaining a) BPA and b) TOC fraction as a function of treatment time for the UVC/H₂O₂ (◇), UVC/S₂O₈²⁻ (△), and UVC/HOCl (□) processes. Conditions: 0.6 mol L⁻¹ of oxidant (flow rate 0.1 mL min⁻¹), pH 3, and 38 °C. Error bars refer to two and three repetitions for the BPA and TOC determinations, respectively.

method was able to quickly (~10 min) oxidize the BPA molecule in the presence of HOCl ($3.2 \pm 0.5 \times 10^{-1} \text{ min}^{-1}$), probably due to the high rates of electrophilic substitution reactions in the aromatic rings of the BPA molecule. Yamamoto & Yasuhara [64] and Lane *et al.* [65] also found fast oxidation reaction of BPA when performing chlorination reaction in neutral to alkaline solutions. As expected for the photochemical and chemical processes, BPA oxidation did not result in significant levels of conversion to CO₂, i.e. mineralization, but only to accumulation of by-products in the reaction medium, as shown in Fig. 1b.

Subsequently, distinct UVC/AOP processes, i.e. H₂O₂, S₂O₈²⁻, and HOCl under UVC irradiation were carried out to assess their performance towards the degradation and mineralization of BPA, as shown in Fig. 2. Clearly, oxidation of the BPA molecule improved significantly when using the UVC/H₂O₂ or UVC/S₂O₈²⁻ methods in relation to their chemical processes, i.e., complete removal was achieved after 300 and 120 min, respectively. This resulted from the activation of these oxidants by the UVC irradiation (particularly at 254 nm) mainly to produce the electrophilic HO[•] and SO₄^{•-} species (see Eqs. (1), 2, and 3), which react with the BPA molecule and its oxidation by-products through addition/abstraction reactions. In the case of the UVC/HOCl method, no significant improvements were observed in the oxidation rate and level as the HOCl species promptly react with the BPA molecule, as previously discussed.

Table 1 presents the values obtained for the pseudo-first order kinetic constants (k_{1st}) regarding the oxidation and mineralization of BPA upon the use of distinct UVC/AOP. As expected, the UVC/HOCl process had higher oxidation rate values ($270 \pm 6 \times 10^{-3} \text{ min}^{-1}$) than the UVC/S₂O₈²⁻ ($35 \pm 2 \times 10^{-3} \text{ min}^{-1}$) and UVC/H₂O₂

Table 1
Pseudo-first order kinetic constants (k_{1st}) for the removal of BPA[†] and TOC^{††} using different UVC/AOP.

Process	k_{1st} (BPA)/10 ⁻³ min ^{-1*}	k_{1st} (TOC)/10 ⁻³ min ^{-1*}
UVC/H ₂ O ₂	15.0 ± 0.3 (0.994)	1.3 ± 0.2 (0.889)
UVC/S ₂ O ₈ ²⁻	35 ± 2 (0.950)	2.3 ± 0.3 (0.870)
UVC/HOCl	270 ± 6 (0.921)	5.8 ± 0.3 (0.938)

[†] mean values obtained after two repetitions.

^{††} mean values obtained after three repetitions.

* The value in parentheses refers to the mean coefficient of determination (R²) of the linear regression carried out to determine the respective value of k_{1st} .

($15 \pm 0.3 \times 10^{-3} \text{ min}^{-1}$) processes. Therefore, for the last two methods, it is clear that the generation of HO^\cdot (and $\text{SO}_4^{\cdot-}$ when using $\text{S}_2\text{O}_8^{2-}$) species might have improved the oxidation towards BPA. Furthermore, the rate constant in UVC/ $\text{S}_2\text{O}_8^{2-}$ is slightly higher than in UVC/ H_2O_2 due to the additional HO^\cdot species generated from reaction of $\text{SO}_4^{\cdot-}$ species with H_2O (see Eq. (3)). Similarly, Sharma *et al.* [36] found that the UVC/ $\text{S}_2\text{O}_8^{2-}$ process ($k_{1st} = 9.4 \times 10^{-3} \text{ min}^{-1}$) is more efficient at BPA oxidation ($[\text{BPA}]_0 = 0.22 \text{ mmol L}^{-1}$) than the UVC/ H_2O_2 process ($k_{1st} = 5.4 \times 10^{-3} \text{ min}^{-1}$). The k_{1st} values achieved ranged one order of magnitude below those found in this work, even when using a 40 W UVC lamp. Sanchez-Polo *et al.* [66] also obtained similar values for k_{1st} ($\sim 10^{-3} \text{ min}^{-1}$) as well as 80% and 70% of BPA oxidation ($[\text{BPA}]_0 = 0.044 \text{ mmol L}^{-1}$) after 180 min for the UVC/ $\text{S}_2\text{O}_8^{2-}$ and UVC/ H_2O_2 methods, respectively, despite using a high power (700 W) mercury medium pressure lamp. The low efficiency towards BPA oxidation reported in these works could be attributed to the self-scavenging reactions of radicals ($\text{SO}_4^{\cdot-}$, HO^\cdot , HO_2^\cdot , $\text{O}_2^{\cdot-}$, etc.) upon a high initial oxidant concentration in solution. Clearly, this issue could be minimized by continuously adding oxidants, as carried out in this study.

For the UVC/HOCl method and its consequent similar removal level and rate as the chemical method using HOCl (see Fig. 1a), it is not clear whether the HO^\cdot and Cl^\cdot species also mediated the oxidation process of the former; however, an analysis of the BPA mineralization (Fig. 2b) reveals the conversion of the produced by-products into CO_2 (90% mineralization after 360 min), which is mainly mediated by HO^\cdot species, as discussed below. These results are more satisfactory than that achieved using the UVC/ H_2O_2 ($\sim 30\%$) and UVC/ $\text{S}_2\text{O}_8^{2-}$ (60%) processes, which is also demonstrated in the calculated rate constants (see Table 1). In addition, all coupled methods had improved performance upon the use of UVC light due to the formation of HO^\cdot and $\text{SO}_4^{\cdot-}$ (when using $\text{S}_2\text{O}_8^{2-}$) species, despite the distinct levels of the tested methods. Sharma *et al.* [36] also reported similar mineralization levels for BPA when using UVC/ H_2O_2 (38%) and UVC/ $\text{S}_2\text{O}_8^{2-}$ (55%) processes after 360 min of treatment.

More recently, researches have applied the UVC/HOCl method to eliminate various CEC (pharmaceuticals, insecticides, herbicides, etc.) [13,67–69]; however, only few works have reported high TOC removal levels, which is an important parameter from the environmental point of view. Yin *et al.* [68] investigated the oxidation of two neonicotinoid insecticides (imidacloprid and thiacloprid) using the UVC/HOCl process (full HOCl addition at the beginning of treatment) for both compounds and reached only $\sim 30\%$ of mineralization in relation to $\sim 90\%$ reported in this study, demonstrating the advantage of continuously adding the HOCl oxidant. In contrast, degradation and mineralization rates obtained in this work corroborate the theoretical kinetic model proposed by Li *et al.* [38], which estimated the performance of these UV-based oxidation technologies. The model predicted that photolysis of the HOCl, $\text{S}_2\text{O}_8^{2-}$, and H_2O_2 oxidants mediated by UVC irradiation (*i.e.* radical production) and their performance towards organics oxidation follows the order: $\text{HOCl} > \text{S}_2\text{O}_8^{2-} > \text{H}_2\text{O}_2$. As expected for the superior oxidation and mineralization of BPA using the HOCl/UVC method, high values (close to 1.0) for the extent of total mineralization (φ) were achieved after 360 min, as shown in Fig. S2 in the supplementary file. Low φ values for the UVC/ $\text{S}_2\text{O}_8^{2-}$ and UVC/ H_2O_2 methods indicate an accumulation of oxidation by-products of BPA in the reaction system.

To better understand the synergistic effect associated with the coupled processes, the experimental curves for the remaining fractions of BPA and TOC as a function of treatment time (t) using the different UVC/AOP processes were compared with the theoretical curves obtained from the summation of the experimental remaining fractions of the photochemical and chemical processes used separately. The experimental and theoretical curves for the remaining fractions of BPA and TOC for the UVC/HOCl, UVC/ H_2O_2 , and UVC/ $\text{S}_2\text{O}_8^{2-}$ processes can be seen in Figs. 3–5, respectively. As above mentioned and due to

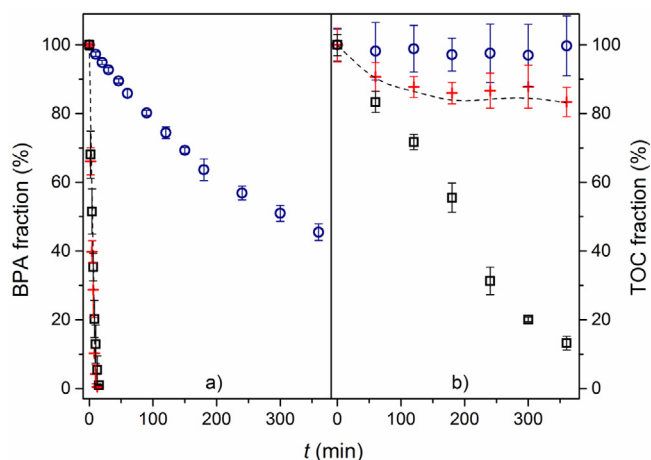


Fig. 3. Remaining a) BPA and b) TOC fraction as a function of treatment time for the, photochemical method (○) chemical method (+), UVC/HOCl process (□), and after summation of the experimental remaining fractions of the photochemical and chemical methods (— —). Conditions: 0.6 mol L^{-1} of oxidant (flow rate 0.1 mL min^{-1}), pH 3, and 38°C . Error bars refer to two and three repetitions for the BPA and TOC determinations, respectively.

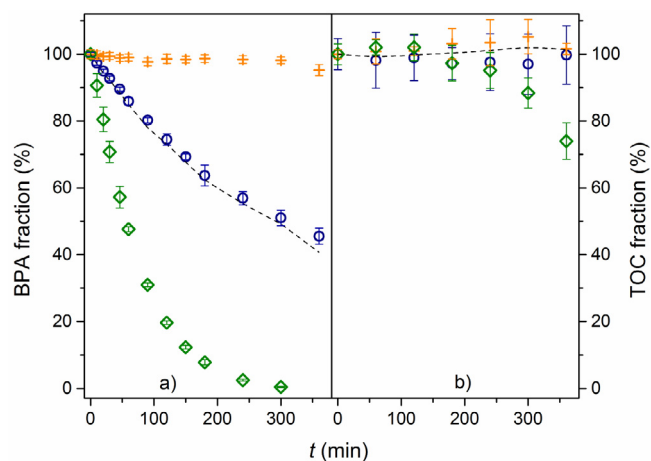


Fig. 4. Remaining fraction of a) BPA and b) TOC as a function of treatment time (t) for the photochemical method (○), chemical method (+), UVC/ H_2O_2 process (◇), and after summation of the experimental photochemical and chemical methods (— —). Conditions: 0.6 mol L^{-1} of oxidant (flow rate 0.1 mL min^{-1}), pH 3, and 38°C . Error bars refer to two and three repetitions for the BPA and TOC determinations, respectively.

the fast BPA oxidation reaction in the presence of HOCl, no synergistic effect resulting from the coupling with UVC irradiation is observed, *i.e.*, the experimental and summation/theoretical lines are coincident. In the case of the UVC/ H_2O_2 (see Fig. 4) and UVC/ $\text{S}_2\text{O}_8^{2-}$ (see Fig. 5) processes, the slope of the experimental line of both methods is higher than the summation line, confirming the synergistic effect of the combined processes. Regarding TOC removal, once again by comparing the experimental and theoretical lines for its remaining fraction, all tested UVC/AOP methods exhibited mineralization removal levels above the results of a simple summation. It clearly suggests the production of $\text{HO}^\cdot/\text{SO}_4^{\cdot-}$ species, which are the main species responsible for converting organic compounds into CO_2 . As the supplementary file shows, a significantly lower concentration of oxidants occurred in the presence of UVC irradiation (see Fig. S3 and its discussion). Such behavior results from the homolysis of oxidants mediated by UVC irradiation that generates HO^\cdot (or $\text{SO}_4^{\cdot-}$) species, which was confirmed with the identification of salicylic acid during the performance of UVC/oxidant experiments in the presence of benzoic acid (see Fig. S4), in addition to

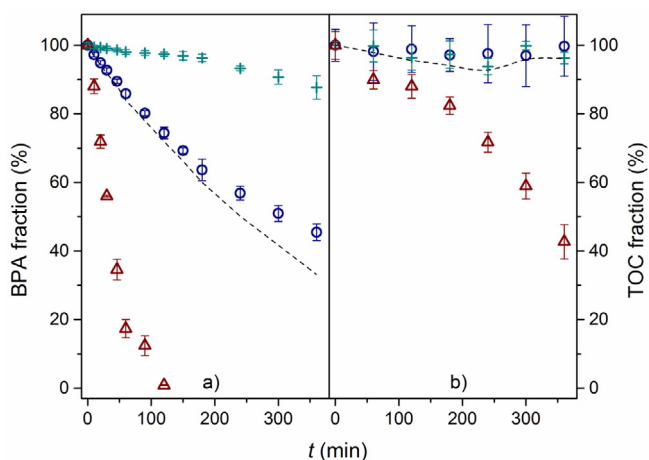


Fig. 5. Remaining fraction of a) BPA and b) TOC as a function of treatment time (t) for the photochemical method (\circ), chemical method ($+$), UVC/S₂O₈²⁻ (\triangle), and after summation of the experimental photochemical and chemical methods ($---$). Conditions: 0.6 mol L⁻¹ of oxidant (flow rate 0.1 mL min⁻¹), pH 3, and 38 °C. Error bars refer to two and three repetitions for the BPA and TOC determinations, respectively.

quenching experiments using isopropanol and tert-butyl alcohol (see Fig. S5 and discussion) for the UVC/S₂O₈²⁻ process.

3.2. Identification of oxidation by-products

In order to identify the main intermediate compounds produced during BPA oxidation using distinct UVC/AOP, aliquots were collected at different treatment time intervals to be analyzed through LC-MS/MS. Table 2 shows the proposed chemical structures for the main oxidation by-products detected, as well as retention times and main fragmentation ions. Among the detected intermediates, only two compounds, n. 3 and n. 4 (m/z 247 and m/z 259, respectively) appeared in all investigated UVC/AOP processes and only compound n. 5 (m/z 261a) occur during treatment of BPA using the UVC/S₂O₈²⁻ and UVC/HOCl processes. Fig. S6, in the supplementary file, illustrates the integrated chromatographic area of the oxidation by-products reported in Table 2 as a function of treatment time. As expected for the UVC/H₂O₂ process, due to its low mineralization levels (see Figs. 2b or 4b) and low φ values, a higher number of oxidation by-products fully hydroxylated were detected, e.g. compounds n. 1, 2, 8, and 9. As far as we could ascertain, this is the first report for the occurrence of these intermediates, except for oxidation by-products 1 and 2, which were found during BPA degradation through the Fenton reaction [70]. In contrast, only three intermediates (3, 4, and 5; two of them with low intensities – see Fig. S6c) occurred for the HOCl/UVC method, which also corroborates the high levels of TOC removal and φ for BPA, as reported earlier. Moreover, and differently from reported in the literature regarding the use of chlorine-based processes for BPA removal [71–73], no organochlorine oxidation by-products were detected during measurements. Such behavior could be attributed to the low accumulation of intermediate compounds, precluding their identification through LC-MS/MS considering the high mineralization rate achieved. In order to confirm the BPA susceptibility regarding the addition of reactions mediated by chlorine species, LC-MS/MS analyses were also carried out for the chemical experiment using only HOCl (i.e., without UVC irradiation). Contrary to the results for the UVC/HOCl process, two organochlorine intermediates (compounds 6 and 7) were detected during the chemical process using HOCl. In addition, throughout the 6 h treatment process the integrated areas for these organochlorine compounds increased (in agreement with the low TOC removed – see Fig. 3), especially for compound 6 (see Fig. S6d), which is more toxic than the parent BPA molecule (see discussion below on the biotoxicity assays). These data

do not imply the absence of chlorination in the BPA molecule during the UVC/HOCl process since the oxidation rate for the chemical and coupled methods were very similar, but it means a possible low amount of organochlorine (probably in the beginning of the reaction and not analyzed in this work, i.e. less than 2 h) completely removed after 6 h of treatment. In contrast, the organochlorine by-products produced during the chemical process using HOCl were detected even after 6 h treatment (see Fig. S6d). In this sense, and to avoid (or minimize) the formation of organochlorine compounds, it is recommended to couple HOCl process and UVC radiation. Figs. S7-S15, in the supplementary file, show the fragmentation route proposed for all intermediates detected. In a general way, most of the oxidation by-products resulted from addition reactions mediated by the electrophilic HO[•] species (as expected for the experiments with benzoic acid) in the methyl substituents and especially in the aromatic rings. The higher polar degree of by-products in relation to the BPA molecule is another characteristic corroborating the proposed oxidation for generating a lower retention time of intermediates during LC-MS/MS as the stationary phase (C-18 column) used is non-polar. The variety of chemical structures identified in this work resulting from hydroxylation reactions confirm the non-selective nature of the HO[•] species (and possibly SO₄^{•-}), as mentioned by other authors [74–77].

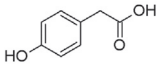
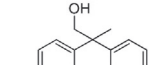
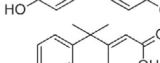
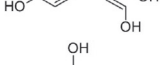
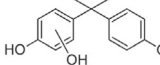
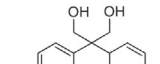
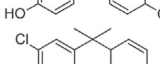
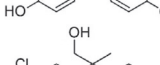
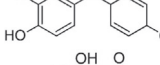
In the final stages of the BPA molecule oxidation, the production of carboxylic acids clearly indicates that the break of aromatic ring and further oxidation before complete mineralization, i.e. conversion to CO₂. In addition, previous studies [78,79] demonstrated that when molecules containing phenolic rings are further oxidized, short chain carboxylic acids, including acetic, formic, fumaric, glyoxylic, maleic, oxalic, and succinic, represented the main detected compounds. In this work, a large number of short chain carboxylic acids (acetic, butyric, dichloroacetic, formic, glycolic, glyoxylic, malic, malonic, oxalic, propionic, pyruvic, succinic, tartaric, and tartronic acids) were identified through HPLC during BPA oxidation. Fig. 6 illustrates the concentration evolution of these carboxylic acids as a function of treatment time using distinct UVC/AOP processes, which shows that the occurrence of tartronic acid for all tested UVC/AOP methods at high concentration values, especially for the UVC/HOCl (~27 mg L⁻¹). This latter method also generated the largest number of carboxylic acids, mainly during the first two hours of experiment; however, almost all were completely removed within 5 h of treatment, even the only chlorinated carboxylic acid detected. Remaining amounts of acetic acid were still detected after 6 h, which might be responsible for the residual TOC values in the final stages of the experiment, as well as other non-identified carboxylic acids. As expected for the chemical process using HOCl, high concentrations of carboxylic acids appeared in the final stages of treatment (mainly acetic, formic, and glyoxylic acids). Moreover and similarly to the treatment using UVC/HOCl, dichloroacetic acid was generated and completely removed within 3 h of treatment (see Fig. S16 in the supplementary file). The UVC/H₂O₂ method produced the highest concentrations of carboxylic acids during the experiment; however, these acids were not completely removed until 6 h of treatment, corroborating the low mineralization levels attained (see Fig. 2b or 4b). Finally, tartronic and glyoxylic acids were the main carboxylic acids produced and detected during treatment using the UVC/S₂O₈²⁻ method. Significantly lower TOC resulted from the complete removal of glyoxylic acid within 3 h of treatment.

3.3. Biototoxicity assays and energy consumption assessment

To assess the environmental compatibility of the UVC/AOP processes, acute toxicity tests using *A. salina* as the testing organism for a 24 h exposure were carried out during the treatment of BPA solutions. The percentage of mortality for *A. salina* decreased during the treatment of BPA solutions and was completely ceased after 4 h with the use of UVC/S₂O₈²⁻ and UVC/HOCl processes, as shown in Fig. 7. In the case of the UVC/H₂O₂ method, the toxicity decreased after 2 h of treatment

Table 2

LC-MS/MS data of the main detected oxidation by-products during treatment of BPA solutions using different UVC/AOP processes.

	Molecular mass (Da)	Retention time (min)	Log K_{ow}^*	Molecular ion $[M-H]^-$ (m/z)	Main fragment ions (m/z)	Proposed chemical structure	Previously reported by ref.
1	152 ^{a‡}	1.86	0.95	151	133 and 107		[70]
2	244 ^{a‡}	1.30	2.2	243	211, 149, and 133		[70]
3	248 ^{abc}	1.16	2.8	247	229, 203, 167, 149, and 119		no
4	260 ^{abc}	1.30	1.7	259	244, 215, 179, and 165		no
5	262a ^{bc}	1.18	1.2	261a	197 and 119		no
6	262b ^d	1.49	4.29	261b	215 and 119		[64]
7	278 ^d	1.56	2.82	277	245, 135, and 119		no
8	324 ^{a†}	1.20	-1.9	323	279, 243, and 227		no
9	342 ^{a†}	1.25	-3.5	341	261 and 243		no

a = UVC/H₂O₂; b = UVC/S₂O₈²⁻; c = UVC/HOCl; d = HOCl.

† only detected in 4 h.

‡ detected in 2 and 4 h.

* values estimated using ECOSAR software.

and had been completely removed by the end of experiment. Considering the 28.9 mg L⁻¹ estimated value for the LC₅₀ for BPA using *A. salina* and the time below 2 h required for the BPA concentration to decrease (see Fig. 2) for all tested UVC/AOP processes, the mortality of *A. salina* was expected to cease just after 2 h of treatment if toxicity occurred only due to the parent molecule. As the time for complete toxicity removal was longer than expected for the LC₅₀ values, treatment of BPA solutions using different UVC/AOP processes result in toxic intermediates whose type and concentration depend on the specific method as well as the complete detoxification of the treated BPA solution.

Pérez-Moya *et al.* [80] reported a sharp mortality decrease using Vero cells after a 5 min treatment of BPA solutions (30 mg L⁻¹) involving Fenton, Fenton-like, and photo-Fenton processes. However, mortality was 50% higher after further reaction time, probably due to the formation of intermediates that are more toxic than the parent molecule. Other authors had found a similar behavior concerning higher toxicity at the beginning of treatment [81].

To benefit the understanding of the results obtained during the toxicity tests using *A. salina*, the ECOSAR software was used to estimate the acute and chronic toxicity baseline of BPA and its oxidation by-products (identified through LC-MS/MS analyses) for different aquatic organisms (*fish*, *daphnid*, and *green algae*). Taking into account the results obtained by using the software and the classification proposed in the Globally Harmonized System of Classification and Labelling of

Chemicals (GHS), as seen in Tables S2 and S3 (in the [supplementary file](#)), respectively, it is possible to state that: *i*) except for the organochlorine compound n. 6, all the remaining oxidation by-products are less toxic than the BPA molecule; *ii*) intermediate compounds n. 1, 4, and 5 are not harmful for acute toxicity, but harmful for chronic toxicity, while intermediate n. 2 is harmful for acute and chronic toxicity – these intermediates were found only during the treatment using the UVC/H₂O₂ process; *iii*) intermediate compound n. 3 is detrimental for acute and chronic toxicity and appeared during all treatment processes; however, its signal during LC-MS/MS analyses was around 15 times higher than when the UVC/H₂O₂ process was used; *iv*) the intermediates identified during the HOCl chemical process, n. 6 and 7, are considered very toxic and toxic toward chronic toxicity, respectively; *v*) the remaining oxidation by-products showed no acute or chronic toxicity effects. All these results may explain why the UVC/H₂O₂ process demanded a prolonged treatment time to reduce toxicity towards *A. salina* in comparison to the UVC/S₂O₈²⁻ and UVC/HOCl processes. In addition, none of the 15 carboxylic acids detected in this work were considered toxic for acute or chronic exposure for the concentration levels obtained and based on the ECOSAR software estimation (data not shown). Among the detected carboxylic acids, glyoxylic acid is considered the most toxic (LC₅₀ = 256 mg L⁻¹) for fish in acute exposure.

An economic comparison to determine the most satisfactory cost-efficiency relationship among the investigated UVC/AOP was performed during BPA oxidation based on the total cost per order (Cost/

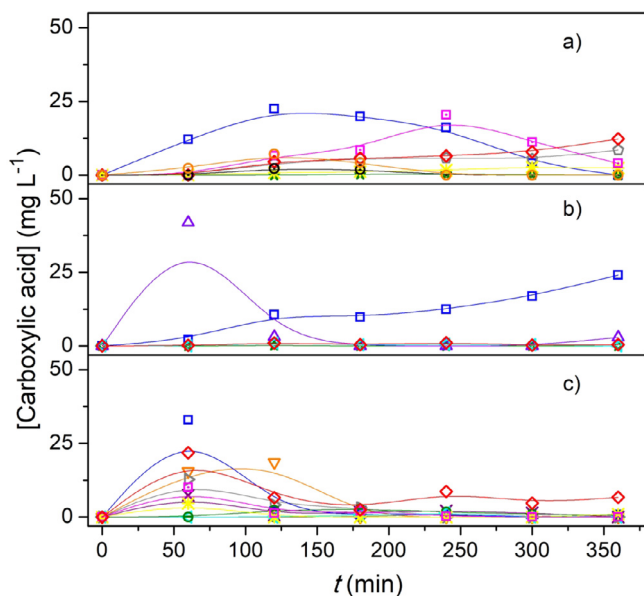


Fig. 6. Concentration evolution of the main detected carboxylic acids as a function of the treatment time for the a) UVC/H₂O₂, b) UVC/S₂O₈²⁻ and c) UVC/HOCl processes: acetic (◇), butyric (○), dichloroacetic (×), formic (□), glycolic (◁), glyoxylic (△), malic (▷), malonic (⊖), oxalic (▽), propionic (⊙), pyruvic (☆), succinic (★), tartaric (▷) and tartronic (◻). Conditions: 0.6 mol L⁻¹ of oxidant (flow rate 0.1 mL min⁻¹), pH 3, and 38 °C.

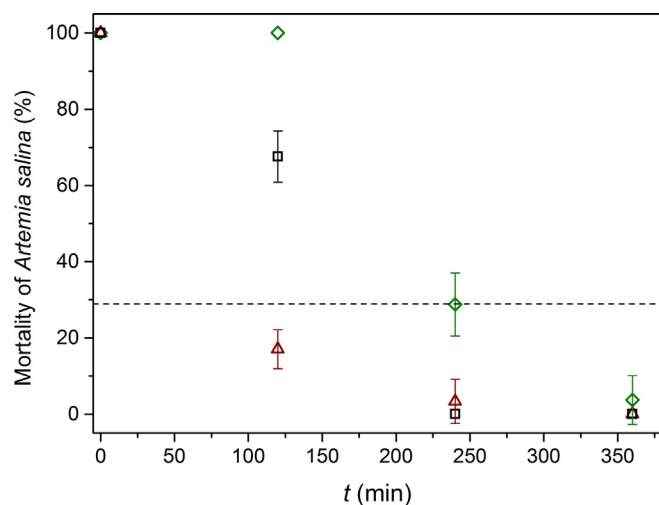


Fig. 7. Evolution of mortality of *A. salina* (%) as a function of the treatment time for the UVC/H₂O₂ (◇), UVC/S₂O₈²⁻ (△), and UVC/HOCl (◻) processes. The dashed line indicates the LC₅₀ value (28.9 mg L⁻¹) found for BPA. The error bars refer to the calculated errors for triplicate analyses. Conditions: 0.6 mol L⁻¹ of oxidant (flow rate 0.1 mL min⁻¹), pH 3, and 38 °C.

O_{TOTAL} · \$ m⁻³ order⁻¹). According to Table 3, the Cost/O_{TOTAL} values proved significantly lower for the UVC/HOCl and UVC/H₂O₂ processes than for the UVC/S₂O₈²⁻ method. Moreover, the Cost/O_{TOTAL} for UVC/HOCl is ~14 times lower than for UVC/H₂O₂ due to the low oxidation rates attained (and low quantum efficiency) through the latter process. In the case of the UVC/S₂O₈²⁻ method, the price of the Na₂S₂O₈ oxidant (Cost/O_{OX}) was higher than the other chemicals, which resulted in higher operational costs. Thus, considering the Cost/O_{TOTAL} parameter, the UVC/S₂O₈²⁻ method is not recommended for BPA oxidation. This result contrasts to the literature reports [82–84], i.e. the UVC/S₂O₈²⁻ process is more cost-efficient method than UVC/H₂O₂, which is clearly related to the lower price of the Na₂S₂O₈ reagent reported in other studies (0.74 \$ kg⁻¹) in relation to ours (13.7 \$ kg⁻¹ from Sigma

Table 3

Economic comparison per order of BPA[†] oxidation using distinct UVC/AOP processes.

Type of cost per order	UVC/H ₂ O ₂	UVC/S ₂ O ₈ ²⁻	UVC/HOCl
Cost/O _{UVC} (\$ m ⁻³ order ⁻¹)	6.87 (3.91)**	3.44 (1.96)**	0.477 (0.272)**
*Cost/O _{OX} (\$ m ⁻³ order ⁻¹)	0.018	1.74	0.018
Cost/O _{TOTAL} (\$ m ⁻³ order ⁻¹)	6.89 (3.93)**	5.18 (3.70)**	0.495 (0.290)**

Experimental conditions: [BPA] = 0.44 mmol L⁻¹, [oxidant] = 0.6 mol L⁻¹ (added in a flow rate of 0.1 mL min⁻¹), pH 3, and 38 °C.

†mean values obtained after two repetitions.

*Oxidant price (US\$): 0.504 kg⁻¹ for H₂O₂ (Synth), 13.7 \$ kg⁻¹ for Na₂S₂O₈ (Sigma Aldrich), and 3.21 kg⁻¹ for NaOCl (Nalgon).

**Values in parentheses refer to calculation taking into account the rated power of the UVC lamp.

Aldrich). Therefore, considering the time of treatment using the UVC lamp and price of chemicals, UVC/HOCl is the most cost-efficient process for BPA oxidation. Lu *et al.* [62] also reported that the UVC/HOCl process is more cost-effective than the UVC/S₂O₈²⁻ method for the oxidation of clofibric acid. In the context of total cost per unit order, an alternative treatment would be the energy consumption per unit mass of removed TOC, as discussed in the supplementary file, see Fig. S17.

Finally, regarding BPA conversion and its oxidation by-products into CO₂, only the UVC/HOCl method was able to remove the content of TOC by one order of magnitude (~90%), therefore, the Cost/O_{TOTAL} value for mineralization using this process remained around 7.8 \$ m⁻³ order⁻¹. Such value is significantly higher (~30 times) than the one for BPA oxidation as the mineralization of complex organic compounds, like BPA and its by-products, requires successive steps of hydroxylation reactions (resulting in a prolonged reaction time). Consequently, there are practically no studies reporting the Cost/O_{TOTAL} for BPA mineralization using UVC/AOP.

4. Conclusion

Among the three investigated UVC/AOP processes in this work, the UVC/HOCl showed the best performance for the oxidation and mineralization of BPA in comparison to the UVC/S₂O₈²⁻ and UVC/H₂O₂ processes. In all methods, UVC irradiation resulted in a significant improvement of the oxidation and mineralization rates and levels due to the homolysis of oxidants and generation of HO[•] and SO₄^{-•} species.

The use of the UVC/HOCl method presented only two hydroxylated intermediates, whereas six oxidation by-products were found during treatment of BPA using UVC/H₂O₂, confirming its lower mineralization extent in relation to the UVC/HOCl method ($\varphi \sim 1$). The LC-MS/MS analyses did not indicate any organochlorine upon the use of the UVC/HOCl process, contrasting to the results from the chemical process. As both processes showed similar BPA oxidation rates, it is speculated that the production of organochlorine intermediates occurs through both methods (UVC/HOCl and HOCl), but are promptly consumed under UVC irradiation through subsequent hydroxylation reactions.

Biotoxicity assays using the *A. salina* crustacean proved effective at showing the toxicity evolution of BPA solutions during the treatment using distinct UVC/AOP. As expected, the mortality of these organisms was completely ceased using the UVC/HOCl treatment process due to the high BPA conversion rate and its intermediates to CO₂. In contrast, a low mortality rate appeared for the UVC/H₂O₂ method, probably due to the oxidation by-products produced as analyzed by comparing between experimental data obtained from the LC-MS/MS analyses and theoretical calculations using the ECOSAR software.

Finally, the UVC/HOCl represents an interesting option for practical applications, like wastewater treatment plants, since high organic removal rates can be achieved under a low operating cost.

Declaration of Competing Interest

The authors declare that they have no known competing financial interests or personal relationships that could have appeared to influence the work reported in this paper.

Acknowledgments

Brazilian funding agencies (*Conselho Nacional de Desenvolvimento Científico e Tecnológico*– CNPq – grant #142350/2016-8 and #141934/2014-0, *Coordenação de Aperfeiçoamento de Pessoal de Nível Superior*–CAPES – Finance Code 001, and *São Paulo Research Foundation* – Fapesp – grants #2008/10449-7 and #2019/07943-4) are gratefully acknowledged for financial support and scholarships. Dr. Hugo César Ramos de Jesus is also acknowledged for the fruitful discussions on the proposed chemical structures.

Appendix A. Supplementary data

Supplementary data to this article can be found online at <https://doi.org/10.1016/j.cej.2019.123986>.

References

- W. Gwenzi, N. Chaukura, Organic contaminants in African aquatic systems: current knowledge, health risks, and future research directions, *Sci. Total Environ.* 619–620 (2018) 1493–1514, <https://doi.org/10.1016/j.scitotenv.2017.11.121>.
- Y. Valcárcel, A. Valdehita, E. Becerra, M. López de Alda, A. Gil, M. Gorga, M. Petrovic, D. Barceló, J.M. Navas, Determining the presence of chemicals with suspected endocrine activity in drinking water from the Madrid region (Spain) and assessment of their estrogenic, androgenic and thyroidal activities, *Chemosphere* 201 (2018) 388–398, <https://doi.org/10.1016/j.chemosphere.2018.02.099>.
- H.-S. Lee, D.-W. Jung, S. Han, H.-S. Kang, J.-H. Suh, H.-S. Oh, M.-S. Hwang, G. Moon, Y. Park, J.-H. Hong, Y.E. Koo, Veterinary drug, 17 β -trenbolone promotes the proliferation of human prostate cancer cell line through the Akt/AR signaling pathway, *Chemosphere* 198 (2018) 364–369, <https://doi.org/10.1016/j.chemosphere.2018.01.145>.
- B. Petrie, R. Barden, B. Kasprzyk-Hordern, A review on emerging contaminants in wastewaters and the environment: current knowledge, understudied areas and recommendations for future monitoring, *Water Res.* 72 (2015) 3–27, <https://doi.org/10.1016/j.watres.2014.08.053>.
- M. Salimi, A. Esrafil, M. Gholami, A. Jonidi Jafari, R. Rezaei Kalantary, M. Farzadkia, M. Kermani, H.R. Sobhi, Contaminants of emerging concern: a review of new approach in AOP technologies, *Environ. Monit. Assess.* 189 (2017) 414, <https://doi.org/10.1007/s10661-017-6097-x>.
- N.H. Tran, M. Reinhard, K.Y.-H. Gin, Occurrence and fate of emerging contaminants in municipal wastewater treatment plants from different geographical regions—a review, *Water Res.* 133 (2018) 182–207, <https://doi.org/10.1016/j.watres.2017.12.029>.
- G. Matafonova, V. Batoev, Recent advances in application of UV light-emitting diodes for degrading organic pollutants in water through advanced oxidation processes: a review, *Water Res.* 132 (2018) 177–189, <https://doi.org/10.1016/j.watres.2017.12.079>.
- G. Boczkaj, A. Fernandes, Wastewater treatment by means of advanced oxidation processes at basic pH conditions: a review, *Chem. Eng. J.* 320 (2017) 608–633, <https://doi.org/10.1016/j.cej.2017.03.084>.
- R. Guan, X. Yuan, Z. Wu, L. Jiang, Y. Li, G. Zeng, Principle and application of hydrogen peroxide based advanced oxidation processes in activated sludge treatment: a review, *Chem. Eng. J.* 339 (2018) 519–530, <https://doi.org/10.1016/j.cej.2018.01.153>.
- S. Waclawek, H.V. Lutze, K. Grübel, V.V.T. Padil, M. Černík, D.D. Dionysiou, Chemistry of persulfates in water and wastewater treatment: a review, *Chem. Eng. J.* 330 (2017) 44–62, <https://doi.org/10.1016/j.cej.2017.07.132>.
- C. Sichel, C. Garcia, K. Andre, Feasibility studies: UV/chlorine advanced oxidation treatment for the removal of emerging contaminants, *Water Res.* 45 (2011) 6371–6380, <https://doi.org/10.1016/j.watres.2011.09.025>.
- J. Jin, M.G. El-Din, J.R. Bolton, Assessment of the UV/chlorine process as an advanced oxidation process, *Water Res.* 45 (2011) 1890–1896, <https://doi.org/10.1016/j.watres.2010.12.008>.
- D.A.C. Coledam, I. Sánchez-Montes, B.F. Silva, J.M. Aquino, On the performance of HOCl/Fe²⁺, HOCl/Fe³⁺/UVA, and HOCl/UVC processes using in situ electro-generated active chlorine to mineralize the herbicide picloram, *Appl. Catal. B Environ.* 227 (2018) 170–177, <https://doi.org/10.1016/j.apcatb.2017.12.072>.
- I.J.S. Montes, B.F. Silva, J.M. Aquino, On the performance of a hybrid process to mineralize the herbicide tebutthiuron using a DSA® anode and UVC light: a mechanistic study, *Appl. Catal. B Environ.* 200 (2017) 237–245, <https://doi.org/10.1016/j.apcatb.2016.07.003>.
- D.B. Miklos, R. Hartl, P. Michel, K.G. Linden, J.E. Drewes, U. Hübner, UV/H₂O₂ process stability and pilot-scale validation for trace organic chemical removal from wastewater treatment plant effluents, *Water Res.* 136 (2018) 169–179, <https://doi.org/10.1016/j.watres.2018.02.044>.
- J.L. Weeks, M.S. Matheson, The primary quantum yield of hydrogen peroxide decomposition, *J. Am. Chem. Soc.* 78 (1956) 1273–1278, <https://doi.org/10.1021/ja01588a002>.
- C.-H. Liao, M.D. Gurol, Chemical oxidation by photolytic decomposition of hydrogen peroxide, *Environ. Sci. Technol.* 29 (1995) 3007–3014, <https://doi.org/10.1021/es00012a018>.
- X.Y. Yu, J.R. Barker, Hydrogen peroxide photolysis in acidic aqueous solutions containing chloride ions. II. Quantum yield of HO(Aq) radicals, *J. Phys. Chem. A* 107 (2003) 1325–1332, <https://doi.org/10.1021/jp026666s>.
- J.C. Crittenden, S. Hu, D.W. Hand, S.A. Green, A kinetic model for H₂O₂/UV process in a completely mixed batch reactor, *Water Res.* 33 (1999) 2315–2328, [https://doi.org/10.1016/S0043-1354\(98\)00448-5](https://doi.org/10.1016/S0043-1354(98)00448-5).
- Q. Yang, H. Choi, Y. Chen, D.D. Dionysiou, Heterogeneous activation of peroxymonosulfate by supported cobalt catalysts for the degradation of 2,4-dichlorophenol in water: the effect of support, cobalt precursor, and UV radiation, *Appl. Catal. B Environ.* 77 (2008) 300–307, <https://doi.org/10.1016/j.apcatb.2007.07.020>.
- F.P. Tully, A.R. Ravishankara, R.L. Thompson, J.M. Nicovich, R.C. Shah, N.M. Kreutter, P.H. Wine, Kinetics of the reactions of hydroxyl radical with benzene and toluene, *J. Phys. Chem.* 85 (1981) 2262–2269, <https://doi.org/10.1021/j150615a025>.
- L. Ebersohn, *Electron-Transfer Reactions in Organic Chemistry*, Springer, Berlin Heidelberg, Berlin, 1987 doi: 10.1007/978-3-642-72544-9.
- W. Da Oh, Z. Dong, T.T. Lim, Generation of sulfate radical through heterogeneous catalysis for organic contaminants removal: current development, challenges and prospects, *Appl. Catal. B Environ.* 194 (2016) 169–201, <https://doi.org/10.1016/j.apcatb.2016.04.003>.
- H. Herrmann, On the photolysis of simple anions and neutral molecules as sources of O[•]/OH, SO₄[•] and Cl in aqueous solution, *Phys. Chem. Chem. Phys.* 9 (2007) 3935–3964, <https://doi.org/10.1039/b618565g>.
- G. Mark, M.N. Schuchmann, H.P. Schuchmann, C. von Sonntag, The photolysis of potassium peroxodisulphate in aqueous solution in the presence of tert-butanol: a simple actinometer for 254 nm radiation, *J. Photochem. Photobiol. A Chem.* 55 (1990) 157–168, [https://doi.org/10.1016/1010-6030\(90\)80028-V](https://doi.org/10.1016/1010-6030(90)80028-V).
- R. Xiao, Z. Luo, Z. Wei, S. Luo, R. Spinney, W. Yang, D.D. Dionysiou, Activation of peroxymonosulfate/persulfate by nanomaterials for sulfate radical-based advanced oxidation technologies, *Curr. Opin. Chem. Eng.* 19 (2018) 51–58, <https://doi.org/10.1016/j.coche.2017.12.005>.
- C. Jiang, Y. Ji, Y. Shi, J. Chen, T. Cai, Sulfate radical-based oxidation of fluoroquinolone antibiotics: kinetics, mechanisms and effects of natural water matrices, *Water Res.* 106 (2016) 507–517, <https://doi.org/10.1016/j.watres.2016.10.025>.
- S. Luo, Z. Wei, D.D. Dionysiou, R. Spinney, W.P. Hu, L. Chai, Z. Yang, T. Ye, R. Xiao, Mechanistic insight into reactivity of sulfate radical with aromatic contaminants through single-electron transfer pathway, *Chem. Eng. J.* 327 (2017) 1056–1065, <https://doi.org/10.1016/j.cej.2017.06.179>.
- J. Szabo, S. Minamyer, Decontamination of biological agents from drinking water infrastructure: a literature review and summary, *Environ. Int.* 72 (2014) 124–128, <https://doi.org/10.1016/j.envint.2014.01.031>.
- T. Uysal, S. Yilmaz, M. Turkoglu, M. Sadikoglu, Investigation of some disinfection chemicals and water quality parameters in swimming pools in the city center and districts of Canakkale, Turkey, *Environ. Monit. Assess.* 189 (2017) 1–13, <https://doi.org/10.1007/s10661-017-6031-2>.
- W. Li, J. Zhang, F. Wang, L. Qian, Y. Zhou, W. Qi, J. Chen, Effect of disinfectant residual on the interaction between bacterial growth and assimilable organic carbon in a drinking water distribution system, *Chemosphere* 202 (2018) 586–597, <https://doi.org/10.1016/j.chemosphere.2018.03.056>.
- Y. Feng, D.W. Smith, J.R. Bolton, Photolysis of aqueous free chlorine species (HOCl and OCl[•]) with 254 nm ultraviolet light, *J. Environ. Eng. Sci.* 6 (2007) 277–284, <https://doi.org/10.1139/s06-052>.
- D.M. Stanbury, *Reduction potentials involving inorganic free radicals in aqueous solution*, in: A.G. Sykes (Ed.), *Advances in Inorganic Chemistry*, Academic Press, San Diego, 1989, pp. 69–138 doi: 10.1016/S0898-8838(08)60194-4.
- Y.H. Chuang, S. Chen, C.J. Chinn, W.A. Mitch, Comparing the UV/monochloramine and UV/free chlorine advanced oxidation processes (AOPs) to the UV/hydrogen peroxide AOP under scenarios relevant to potable reuse, *Environ. Sci. Technol.* 51 (2017) 13859–13868, <https://doi.org/10.1021/acs.est.7b03570>.
- J. Fang, Y. Fu, C. Shang, The roles of reactive species in micropollutant degradation in the UV/free chlorine system, *Environ. Sci. Technol.* 48 (2014) 1859–1868, <https://doi.org/10.1021/es4036094>.
- J. Sharma, I.M. Mishra, V. Kumar, Degradation and mineralization of bisphenol A (BPA) in aqueous solution using advanced oxidation processes: UV/H₂O₂ and UV/S₂O₈²⁻ oxidation systems, *J. Environ. Manage.* 156 (2015) 266–275, <https://doi.org/10.1016/j.jenvman.2015.03.048>.
- A.A. Babaei, F. Ghanbari, COD removal from petrochemical wastewater by UV/hydrogen peroxide, UV/persulfate and UV/percarbonate: biodegradability improvement and cost evaluation, *J. Water Reuse Desalin.* 6 (2016) 484–494, <https://doi.org/10.2166/wrd.2016.188>.
- W. Li, T. Jain, K. Ishida, H. Liu, A mechanistic understanding of the degradation of trace organic contaminants by UV/hydrogen peroxide, UV/persulfate and UV/free chlorine for water reuse, *Environ. Sci. Water Res. Technol.* 3 (2017) 128–138, <https://doi.org/10.1039/C6EW00242K>.
- X. Ao, W. Liu, Degradation of sulfamethoxazole by medium pressure UV and oxidants: peroxymonosulfate, persulfate, and hydrogen peroxide, *Chem. Eng. J.* 313

- (2017) 629–637, <https://doi.org/10.1016/j.ccej.2016.12.089>.
- [40] G.V. Buxton, C.L. Greenstock, W.P. Helman, A.B. Ross, Critical review of rate constants for reactions of hydrated electrons, hydrogen atoms and hydroxyl radicals ($\cdot\text{OH}/\cdot\text{O}^-$) in aqueous solution, *J. Phys. Chem. Ref. Data* 17 (1988) 513–886, <https://doi.org/10.1063/1.555805>.
- [41] G. Beck, Elektrische nachweis geladener zwischenprodukte pulsradiolyse, *Int. J. Radiat. Phys. Chem.* 1 (1969) 361–371, [https://doi.org/10.1016/0020-7055\(69\)90033-3](https://doi.org/10.1016/0020-7055(69)90033-3).
- [42] K. Sehested, O.L. Rasmussen, H. Fricke, Rate constants of OH with HO_2 , O_2^- , and H_2O_2^+ from hydrogen peroxide formation in pulse-irradiated oxygenated water, *J. Phys. Chem.* 72 (1968) 626–631, <https://doi.org/10.1021/j100848a040>.
- [43] G.V. Buxton, M. Bydder, G. Arthur Salmon, The reactivity of chlorine atoms in aqueous solution Part II. The equilibrium $\text{SO}_4^{\cdot-} + \text{Cl}^- \rightleftharpoons \text{Cl}^\cdot + \text{SO}_4^{2-}$, *Phys. Chem. Chem. Phys.* 1 (1999) 269–273, <https://doi.org/10.1039/a807808d>.
- [44] R.E. Huie, C.L. Clifton, Rate constants for hydrogen abstraction reactions of the sulfate radical, $\text{SO}_4^{\cdot-}$. Alkanes and ethers, *Int. J. Chem. Kinet.* 21 (1989) 611–619, <https://doi.org/10.1002/kin.550210802>.
- [45] E. Hayon, A. Treinin, J. Wilf, Electronic spectra, photochemistry, and autoxidation mechanism of the sulfite-bisulfite-pyrosulfite systems. SO_2^- , SO_3^- , SO_4^- , and SO_5^- radicals, *J. Am. Chem. Soc.* 94 (1972) 47–57, <https://doi.org/10.1021/ja00756a009>.
- [46] C.A. Ennis, J.W. Birks, Rate constants for the reactions $\text{OH} + \text{HOCl} \rightarrow \text{H}_2\text{O} + \text{ClO}$ and $\text{H} + \text{HOCl} \rightarrow \text{products}$, *J. Phys. Chem.* 92 (1988) 1119–1126, <https://doi.org/10.1021/j100316a024>.
- [47] G.G. Jayson, B.J. Parsons, A.J. Swallow, Some simple, highly reactive, inorganic chlorine derivatives in aqueous solution. Their formation using pulses of radiation and their role in the mechanism of the Fricke dosimeter, *J. Chem. Soc., Faraday Trans. 1* 69 (0) (1973) 1597–1607, <https://doi.org/10.1039/f19736901597>.
- [48] C. Liang, C. Huang, N. Mohanty, R.M. Kurakalva, A rapid spectrophotometric determination of persulfate anion in ISCO, *Chemosphere* 73 (2008) 1540–1543, <https://doi.org/10.1016/j.chemosphere.2008.08.043>.
- [49] X.-S. Chai, Q. Hou, Q. Luo, J. Zhu, Rapid determination of hydrogen peroxide in the wood pulp bleaching streams by a dual-wavelength spectroscopic method, *Anal. Chim. Acta* 507 (2004) 281–284, <https://doi.org/10.1016/j.aca.2003.11.036>.
- [50] D.A.C. Coledam, J.M. Aquino, B.F. Silva, A.J. Silva, R.C. Rocha-Filho, Electrochemical mineralization of norfloxacin using distinct boron-doped diamond anodes in a filter-press reactor, with investigations of toxicity and oxidation by-products, *Electrochim. Acta* 213 (2016) 856–864, <https://doi.org/10.1016/j.electacta.2016.08.003>.
- [51] R. Guerra, Ecotoxicological and chemical evaluation of phenolic compounds in industrial effluents, *Chemosphere* 44 (2001) 1737–1747, [https://doi.org/10.1016/S0045-6535\(00\)00562-2](https://doi.org/10.1016/S0045-6535(00)00562-2).
- [52] M. Punzi, F. Nilsson, A. Anbalagan, B.M. Svensson, K. Jönsson, B. Mattiasson, M. Junstrup, Combined anaerobic-ozonation process for treatment of textile wastewater: removal of acute toxicity and mutagenicity, *J. Hazard. Mater.* 292 (2015) 52–60, <https://doi.org/10.1016/j.jhazmat.2015.03.018>.
- [53] P. Vanhaecke, G. Persoone, C. Claus, P. Sorgeloos, Proposal for a short-term toxicity test with *Artemia nauplii*, *Ecotoxicol. Environ. Saf.* 5 (1981) 382–387, [https://doi.org/10.1016/0147-6513\(81\)90012-9](https://doi.org/10.1016/0147-6513(81)90012-9).
- [54] J.M. Aquino, G.F. Pereira, R.C. Rocha-Filho, N. Bocchi, S.R. Biaggio, Combined coagulation and electrochemical process to treat and detoxify a real textile effluent, *Water. Air. Soil Pollut.* 227 (2016) 266, <https://doi.org/10.1007/s11270-016-2967-z>.
- [55] M.A. Hamilton, R.C. Russo, R.V. Thurston, Trimmed Spearman-Kärber method for estimating median lethal concentrations in toxicity bioassays, *Environ. Sci. Technol.* 11 (1977) 714–719, <https://doi.org/10.1021/es60130a004>.
- [56] V.G. Beretsou, A.K. Psoma, P. Gago-Ferrero, R. Aalizadeh, K. Fenner, N.S. Thomaidis, Identification of biotransformation products of citalopram formed in activated sludge, *Water Res.* 103 (2016) 205–214, <https://doi.org/10.1016/j.watres.2016.07.029>.
- [57] N. Burden, S.K. Maynard, L. Weltje, J.R. Wheeler, The utility of QSARs in predicting acute fish toxicity of pesticide metabolites: a retrospective validation approach, *Regul. Toxicol. Pharmacol.* 80 (2016) 241–246, <https://doi.org/10.1016/j.yrtph.2016.05.032>.
- [58] I. Carpinteiro, R. Rodil, J.B. Quintana, R. Cela, Reaction of diazepam and related benzodiazepines with chlorine. kinetics, transformation products and in-silico toxicological assessment, *Water Res.* 120 (2017) 280–289, <https://doi.org/10.1016/j.watres.2017.04.063>.
- [59] Y. Yang, X. Lu, J. Jiang, J. Ma, G. Liu, Y. Cao, W. Liu, J. Li, S. Pang, X. Kong, C. Luo, Degradation of sulfamethoxazole by UV, UV/H₂O₂ and UV/persulfate (PDS): formation of oxidation products and effect of bicarbonate, *Water Res.* 118 (2017) 196–207, <https://doi.org/10.1016/j.watres.2017.03.054>.
- [60] R. Zhang, Y. Yang, C.-H. Huang, N. Li, H. Liu, L. Zhao, P. Sun, UV/H₂O₂ and UV/PDS treatment of trimethoprim and sulfamethoxazole in synthetic human urine: transformation products and toxicity, *Environ. Sci. Technol.* 50 (2016) 2573–2583, <https://doi.org/10.1021/acs.est.5b05604>.
- [61] D.W. Miwa, G.R.P. Malpass, S.A.S. Machado, A.J. Motheo, Electrochemical degradation of carbaryl on oxide electrodes, *Water Res.* 40 (2006) 3281–3289, <https://doi.org/10.1016/j.watres.2006.06.033>.
- [62] X. Lu, Y. Shao, N. Gao, J. Chen, H. Deng, W. Chu, N. An, F. Peng, Investigation of cloffibric acid removal by UV/persulfate and UV/chlorine processes: kinetics and formation of disinfection byproducts during subsequent chlor(am)ination, *Chem. Eng. J.* 331 (2018) 364–371, <https://doi.org/10.1016/j.ccej.2017.08.117>.
- [63] J.R. Bolton, K.G. Bircher, W. Tumas, C.A. Tolman, Figures-of-merit for the technical development and application of advanced oxidation technologies for both electric- and solar-driven systems (IUPAC Technical Report), *Pure Appl. Chem.* 73 (2001) 627–637, <https://doi.org/10.1351/pac200173040627>.
- [64] T. Yamamoto, A. Yasuhara, Chlorination of bisphenol A in aqueous media: formation of chlorinated bisphenol A congeners and degradation to chlorinated phenolic compounds, *Chemosphere* 46 (2002) 1215–1223, [https://doi.org/10.1016/S0045-6535\(01\)00198-9](https://doi.org/10.1016/S0045-6535(01)00198-9).
- [65] R.F. Lane, C.D. Adams, S.J. Randtke, R.E. Carter, Chlorination and chloramination of bisphenol A, bisphenol F, and bisphenol A diglycidyl ether in drinking water, *Water Res.* 79 (2015) 68–78, <https://doi.org/10.1016/j.watres.2015.04.014>.
- [66] M. Sánchez-Polo, M.M. Abdel daiem, R. Ocampo-Pérez, J. Rivera-Utrilla, A.J. Mota, Comparative study of the photodegradation of bisphenol A by HO \cdot , SO $_4^{\cdot-}$ and CO $_3^{\cdot-}$ /HCO $_3^{\cdot-}$ radicals in aqueous phase, *Sci. Total Environ.* 463–464 (2013) 423–431, <https://doi.org/10.1016/j.scitotenv.2013.06.012>.
- [67] Y.U. Zhu, M. Wu, N. Gao, W. Chu, K. Li, S. Chen, Degradation of phenacetin by the UV/chlorine advanced oxidation process: kinetics, pathways, and toxicity evaluation, *Chem. Eng. J.* 335 (2018) 520–529, <https://doi.org/10.1016/j.ccej.2017.10.070>.
- [68] K. Yin, Y. Deng, C. Liu, Q. He, Y. Wei, S. Chen, T. Liu, S. Luo, Kinetics, pathways and toxicity evaluation of neonicotinoid insecticides degradation via UV/chlorine process, *Chem. Eng. J.* 346 (2018) 298–306, <https://doi.org/10.1016/j.ccej.2018.03.168>.
- [69] X. Kong, J. Jiang, J. Ma, Y. Yang, W. Liu, Y. Liu, Degradation of atrazine by UV/chlorine: efficiency, influencing factors, and products, *Water Res.* 90 (2016) 15–23, <https://doi.org/10.1016/j.watres.2015.11.068>.
- [70] J. Poerschmann, U. Trommler, T. Górecki, Aromatic intermediate formation during oxidative degradation of bisphenol A by homogeneous sub-stoichiometric Fenton reaction, *Chemosphere* 79 (2010) 975–986, <https://doi.org/10.1016/j.chemosphere.2010.03.030>.
- [71] H. Li, Y. Long, Y. Wang, C. Zhu, J. Ni, Electrochemical degradation of bisphenol A in chloride electrolyte — factor analysis and mechanisms study, *Electrochim. Acta* 222 (2016) 1144–1152, <https://doi.org/10.1016/j.electacta.2016.11.086>.
- [72] H. Li, Y. Long, X. Zhu, Y. Tian, J. Ye, Influencing factors and chlorinated byproducts in electrochemical oxidation of bisphenol A with boron-doped diamond anodes, *Electrochim. Acta* 246 (2017) 1121–1130, <https://doi.org/10.1016/j.electacta.2017.06.163>.
- [73] A. Outsouk, Z. Frontistis, R.S. Ribeiro, M. Antonopoulou, I.K. Konstantinou, A.M.T. Silva, J.L. Faria, H.T. Gomes, D. Mantzavinos, Activation of sodium persulfate by magnetic carbon xerogels (CX/CoFe) for the oxidation of bisphenol A: process variables effects, matrix effects and reaction pathways, *Water Res.* 124 (2017) 97–107, <https://doi.org/10.1016/j.watres.2017.07.046>.
- [74] M. Rajab, C. Heim, T. Letzel, J.E. Drewes, B. Helmreich, Oxidation of bisphenol A by a boron-doped diamond electrode in different water matrices: transformation products and inorganic by-products, *Int. J. Environ. Sci. Technol.* 13 (2016) 2539–2548, <https://doi.org/10.1007/s13762-016-1087-z>.
- [75] F.D. Koppinke, A. Georgi, What controls selectivity of hydroxyl radicals in aqueous solution? Indications for a cage effect, *J. Phys. Chem. A* 121 (2017) 7947–7955, <https://doi.org/10.1021/acs.jpca.7b05782>.
- [76] E. Mousset, N. Oturan, M.A. Oturan, An unprecedented route of $\cdot\text{OH}$ radical reactivity evidenced by an electrocatalytic process: ipso-substitution with perhalogenocarbon compounds, *Appl. Catal. B Environ.* 226 (2018) 135–146, <https://doi.org/10.1016/j.apcatb.2017.12.028>.
- [77] S. Garcia-Segura, E. Brillas, Applied photoelectrocatalysis on the degradation of organic pollutants in wastewaters, *J. Photochem. Photobiol. C Photochem. Rev.* 31 (2017) 1–35, <https://doi.org/10.1016/j.jphotochemrev.2017.01.005>.
- [78] W. Chu, C. Kwan, K. Chan, S. Kam, A study of kinetic modelling and reaction pathway of 2,4-dichlorophenol transformation by photo-Fenton-like oxidation, *J. Hazard. Mater.* 121 (2005) 119–126, <https://doi.org/10.1016/j.jhazmat.2005.01.019>.
- [79] M. Molkenhain, T. Olmez-Hanci, M.R. Jekel, I. Arslan-Alaton, Photo-Fenton-like treatment of BPA: effect of UV light source and water matrix on toxicity and transformation products, *Water Res.* 47 (2013) 5052–5064, <https://doi.org/10.1016/j.watres.2013.05.051>.
- [80] M. Pérez-Moya, T. Kaisto, M. Navarro, L.J. del Valle, Study of the degradation performance (TOC, BOD, and toxicity) of bisphenol A by the photo-Fenton process, *Environ. Sci. Pollut. Res.* 24 (2017) 6241–6251, <https://doi.org/10.1007/s11356-016-7386-6>.
- [81] N. Lu, Y. Lu, F. Liu, K. Zhao, X. Yuan, Y. Zhao, Y. Li, H. Qin, J. Zhu, H₃PW₁₂O₄₀/TiO₂ catalyst-induced photodegradation of bisphenol A (BPA): kinetics, toxicity and degradation pathways, *Chemosphere* 91 (2013) 1266–1272, <https://doi.org/10.1016/j.chemosphere.2013.02.023>.
- [82] J.A. Khan, X. He, N.S. Shah, H.M. Khan, E. Hapeshi, D. Fatta-Kassinos, D.D. Dionysiou, Kinetic and mechanism investigation on the photochemical degradation of atrazine with activated H₂O₂, S₂O₈²⁻ and HSO₅⁻, *Chem. Eng. J.* 252 (2014) 393–403, <https://doi.org/10.1016/j.ccej.2014.04.104>.
- [83] J. Deng, Y. Shao, N. Gao, S. Xia, C. Tan, S. Zhou, X. Hu, Degradation of the anti-epileptic drug carbamazepine upon different UV-based advanced oxidation processes in water, *Chem. Eng. J.* 222 (2013) 150–158, <https://doi.org/10.1016/j.ccej.2013.02.045>.
- [84] Y. Xiao, L. Zhang, W. Zhang, K.-Y. Lim, R.D. Webster, T.-T. Lim, Comparative evaluation of iodoacids removal by UV/persulfate and UV/H₂O₂ processes, *Water Res.* 102 (2016) 629–639, <https://doi.org/10.1016/j.watres.2016.07.004>.